Thermodynamic and Structural Analysis of Phosphotyrosine Polypeptide Binding to Grb2-SH2

Charles McNemar, Mark E. Snow, William T. Windsor,* Andrew Prongay, Philip Mui, Rumin Zhang, James Durkin, Hung V. Le, and Patricia C. Weber

Structural Chemistry Department, Schering-Plough Research Institute, 2015 Galloping Hill Road, Kenilworth, New Jersey 07033

Received February 25, 1997; Revised Manuscript Received June 2, 1997[⊗]

ABSTRACT: A thermodynamic analysis using isothermal titration calorimetry (ITC) has been performed to examine the binding interaction between the SH2 (*Src* homology 2) domain of growth factor receptor binding protein 2 (Grb2-SH2) and one of its phosphotyrosine (pY) polypeptide ligands. Interaction of the Shc-derived phosphotyrosine hexapeptide Ac-SpYVNVQ-NH_2 with Grb2-SH2 was both enthalpically and entropically favorable ($\Delta H = -7.55$ kcal mol^{-1}, $-T\Delta S = -1.46$ kcal mol^{-1} , $\Delta G = -9.01$ kcal mol^{-1}, $T = 20$ °C). ITC experiments using five alanine-substituted peptides were performed to examine the role of each side chain in binding. The results were consistent with homology models of the Grb2-SH2−Shc hexapeptide complex which identified several possible hydrogen bonds between Grb2-SH2 and the phosphotyrosine and conserved asparagine(+2) side chains of the Shc hexapeptide. These studies also demonstrated that the hydrophobic valine(+1) side chain contributes significantly to the favorable entropic component of binding. The thermodynamic and structural data are consistent with a Grb2-SH2 recognition motif of pY-hydrophobic-N-X (where X is any amino acid residue). The measured heat capacity of binding ($\Delta C_p = -146$ cal mol^{-1} K^{-1}) was very similar to computed values using semiempirical estimates ($\Delta C_p = -106$ to -193 cal mol^{-1} K^{-1}) derived from apolar and polar accessible surface area values calculated from several homology models of the Grb2-SH2−Shc hexapeptide complex. The homology model which most closely reproduced the measured ΔC_p value is also the model which had the lowest RMS deviation from the subsequently determined crystal structure. Calculations based on the thermodynamic data and these semiempirical estimates indicated that the binding event involves burial of nearly comparable apolar (677 Å^2) and polar (609 Å^2) surface areas.

Src homology 2 (SH2)[1] domains are modular components of intracellular proteins which promote signal transduction from the plasma membrane through the cytoplasm to the nucleus. Signaling is achieved by SH2 recognition of phosphotyrosine- (pY) containing sequences on a variety of activated proteins (Sadowsky *et al.*, 1986). Structural studies of several SH2 domains both with and without bound peptide reveal a highly conserved three-dimensional fold (Waksman *et al.*, 1992, 1993; Eck *et al.*, 1993; Pascal *et al.*, 1994; Lee *et al.*, 1994a; Xu *et al.*, 1995). The ∼100 residue SH2 domains also possess similar features for the recognition of the phosphotyrosine-containing peptide. The SH2 domain−pY interaction is stabilized by a network of hydrogen bonds arising from conserved arginine, serine, and threonine side chains and peptide backbone atoms. In addition to interactions with the pY residue, peptide recognition also involves three to four additional residues on the C-terminal side of the pY (pY-X-X-X) (Pawson & Schlessinger, 1993; Pawson, 1995). SH2 domains can be classified by the type of residue preferred at each position of the polypeptide ligand (Songyang *et al.*, 1993, 1994). For example, the class I *Src* kinase SH2 domain family recognizes polypeptides containing pY-hydrophilic-hydrophilic-hydrophobic residues, while class III SH2 domains such as *Syp* require motifs containing pY-hydrophobic-X-hydrophobic (where X represents any residue).

Several groups have recently used isothermal titration calorimetry (ITC) to examine the interaction between pY peptide ligands and SH2 domain proteins. Lemmon and Ladbury (1994) determined the affinity and thermodynamic binding parameters for several phosphotyrosine-containing ligands binding to the $p56^{lck}$ (*lck*) SH2 domain. These different peptides bound with a similar change in free energy ($\Delta G \sim -7.0$ kcal mol^{-1}, $K_d \sim 5$ μM); however, the enthalpic and entropic contributions to binding were very different. Ligand binding to either the isolated SH2 domain or an extended construct containing both the SH2 and SH3 domains (SH2−SH3) gave similar ΔG values, indicating that peptide binding to the SH2 domain is relatively independent of other domains in the protein. ITC studies performed with pY peptide ligands and the SH2 domains from *Src* and p85 detected larger ΔG values, ~ -8.6 kcal mol^{-1} ($K_d \sim 0.5$ μM; Ladbury *et al.*, 1995) and correspondingly larger favorable enthalpic contributions ($\Delta H \sim -9$ kcal mol^{-1}). The thermodynamic information obtained from these initial ITC binding studies has provided a framework from which more detailed studies can be designed.

* Send correspondence to this author at Schering-Plough Research Institute, K15-2-2945, Kenilworth, NJ 07033: telephone, (908) 298-3429; FAX, (908) 298-4844; email, william.windsor@spcorp.com.

[⊗] Abstract published in *Advance ACS Abstracts,* August 1, 1997.

[1] Abbreviations: ITC, isothermal titration calorimetry; SH2, *Src* homology domain; Grb2-SH2, growth factor receptor binding protein 2; SH3, *Src* homology domain 3; pY, phosphotyrosine; pY317, Ac-S(pY)VNVQ-NH_2; S(−1)A, Ac-**A**(pY)VNVQ-NH_2; V(+1)A, Ac-S(pY)**A**NVQ-NH_2; N(+2)A, Ac-S(pY)V**A**VQ-NH_2; V(+3)A, Ac-S(pY)VN**A**Q-NH_2; Q(+4)A, Ac-S(pY)VNV**A**-NH_2; ASA, accessible surface area.

S0006-2960(97)00436-4 CCC: $14.00

Here we report ITC and homology modeling studies undertaken to deconvolute the thermodynamic contributions of each side chain involved in pY polypeptide binding to the SH2 domain of growth factor receptor protein 2 (Grb2). Grb2, an adapter protein consisting of one SH2 domain and two *Src* homology 3 (SH3) domains, is critical for promoting signal transduction from epidermal growth factor, platelet-derived growth factor, fibroblast growth factors, and insulin (Lowenstein *et al*., 1992; Ward *et al*., 1996; Skolnik *et al*., 1993; Rozakis-Adcock *et al*., 1992). The SH2 domain binds to phosphotyrosine regions on either the C-terminal end of epidermal growth factor receptor (EGF-R) (binding sites: EpY_{1068}INQS, EpY_{1114}LNTV) or to the receptor-bound Shc protein (binding site: SpY_{317}VNVQ) (Ward *et al*., 1996; Skolnik *et al*., 1993; Rozakis-Adcock *et al*., 1993). The SH3 domains of Grb2 also bind the nucleotide exchange factor Son of sevenless (Sos) protein (Egan *et al*., 1993; Li *et al*., 1993). The receptor-facilitated membrane proximal location of the Grb2−Sos complex enables Sos to associate and activate the plasma membrane associated $p21^{ras}$ (Ras) G protein by exchanging GDP for GTP. Activation of Ras stimulates the MAP kinase cascade, allowing signal transduction from the cell surface receptors to the nucleus where cell proliferation and differentiation are initiated. Uncontrolled cell proliferation and tumor formation resulting from the expression of oncogene ligands such as that reported for Shc and the fusion protein BCR-Abl, which has been linked to chronic myeloid leukemia, might be blocked if the interactions between the Grb2-SH2 domain and its pY ligands are inhibited (Pendergast *et al*., 1993; Maru *et al*., 1995, Maru *et al.*, 1996).

The ligand specificity of the Grb2-SH2 domain significantly differs from that of the *Src* or *lck* SH2 domains. The Grb2-SH2 consensus recognition sequence is pY-X-N-X, where the specificity site is located at the second residue instead of the third residue C-terminal to the pY as observed for the *Src* SH2 domain (Songyang *et al*., 1994; Ward *et al*., 1996). To elucidate the role of each peptide residue in complex formation between the Grb2-SH2 domain and peptide ligand, an extensive thermodynamic analysis of this interaction was performed. Isothermal titration calorimetric measurements using the native Shc ligand, Ac-SpYVNVQ-NH_2, and five different alanine-substituted polypeptides were conducted, and here we report values for the changes in free energy of binding (ΔG), enthalpy (ΔH), and entropy (ΔS) for each ligand. The heat of ionization (ΔH_{ion}) was also determined to deconvolute the enthalpy of binding from buffer-related protonation and deprotonation reactions coupled to complexation.

Grb2-SH2 homology models were constructed for visual inspection of the interactions and to provide a framework for computation of thermodynamic binding parameters. The homology models, based on the known structures of *Src* and *Syp*, were built using three different homology modeling methods. From these structures, semiempirical calculations were performed to estimate the heat capacity, enthalpies, and entropies of binding using several methodologies (Murphy & Freire, 1992; Spolar *et al*., 1992; Murphy *et al*., 1993; Gomez & Freire, 1995; Myers *et al*., 1995). Here we compare the calculated values to those determined by isothermal titration calorimetry and suggest that this comparison is helpful in the identification of more native-like homology models.

MATERIALS AND METHODS

Grb2-SH2. The DNA construct for the Grb2-SH2 domain contained the primary amino acid sequence 53−163 and was expressed in *Escherichia coli* (SG1309,lon$^-$) using a T5 promoter on plasmid QE60 (Lowenstein *et al.*, 1992). The cells were grown to an OD600 of 1.0 and then induced for 4 h with 1 mM IPTG. The cells were harvested by centrifugation, resuspended in buffer A (25 mM Tris and 25 mM NaCl, pH 7.5) containing a protease inhibitor cocktail (0.5 μg/mL Pefabloc, 0.5 μg/mL Leupeptin, 0.7 μg/mL pepstatin A, 2 μg/mL aprotinin, 1.0 μg/mL E64, and 1 mM EDTA), and lysed in a microfluidizer. Following centrifugation of the cell lysate, the supernatant containing soluble Grb2-SH2 was applied to a phosphotyrosine−agarose column, which was then washed with buffer A and eluted with buffer B (25 mM Tris and 200 mM NaCl, pH 7.5). Fractions containing Grb2-SH2 were concentrated and applied to a Mono-Q column (Pharmacia, Piscataway, NJ). The column was washed with buffer B, and the Grb2-SH2 samples (>95% pure) were recovered from the unbound fractions. These fractions were dialyzed against 50 mM HEPES, pH 7.0, loaded onto a Mono-S column (Pharmacia, Piscataway, NJ), and eluted with a 0−500 mM NaCl gradient. The Grb2-SH2 samples eluting at ∼180 mM NaCl were >98% pure, based on SDS−PAGE Coomassie-stained gels and amino acid composition analysis. The extinction coefficient, determined from its absorbance spectrum and a concentration determination from amino acid analysis, is $\epsilon(280) = 1.2$ mg^{-1} cm^2 (15 600 M^{-1} cm^{-1}).

Peptides. Peptides were synthesized in our laboratory or by AnaSpec Inc. (San Jose, CA) using Fmoc solid-phase peptide synthesis with the following protecting groups: *tert*-butyl for serine and tyrosine, and trityl for asparagine and glutamine. Fmoc-phosphotyrosine was used without side chain protection. Peptide N- and C-termini were capped with acetate and amide groups, respectively. Peptide sequences were confirmed by mass spectrometry and amino acid analysis. An extinction coefficient for each peptide was determined from the absorbance at 280 nm and the peptide concentration determined by amino acid analysis. Extinction coefficient values ranged between 600 and 700 M^{-1} cm^{-1}, and are approximately half the value for an L-tyrosine residue at pH 7.0. The following are the primary sequence and code for each peptide used in this study: native sequence pY317, Ac-S(pY)VNVQ-NH_2; alanine substitutions S(−1)A, Ac-**A**(pY)VNVQ-NH_2; V(+1)A, Ac-S(pY)**A**NVQ-NH_2; N(+2)A, Ac-S(pY)V**A**VQ-NH_2; V(+3)A, Ac-S(pY)VN**A**Q-NH_2; Q(+4)A, Ac-S(pY)VNV**A**-NH_2.

Isothermal Titration Calorimetry. Titrations were performed using a MCS isothermal titration calorimeter (MicroCal Corp. Northampton, MA) (Wiseman *et al*., 1989). Grb2-SH2 was dialyzed overnight with two exchanges of buffer (1/1000 v/v). To reduce errors arising from heats of dilution due to buffer differences between samples in the syringe and the stirred vessel, the lyophilized peptide ligands were suspended in the dialysate from the Grb2-SH2 sample. Protein samples were routinely centrifuged, and both peptide and protein solutions were degassed prior to loading into the syringe and reaction cell. Protein and peptide concentrations were determined using measured A_{280} values and the extinction coefficients described above. Peptide ligands (100−250 μM) were titrated into the protein-containing sample cell using a 250 μL syringe. Binding curves usually

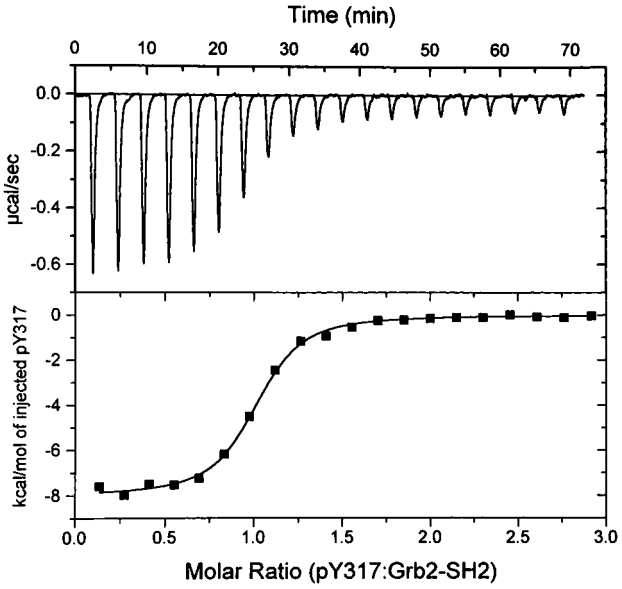

FIGURE 1: (Top) Exothermic heats of reaction (μcal/s) measured for 20 injections of the pY317 peptide into a Grb2-SH2 sample. Ten microliter additions of pY317 (250 μM) were injected into a 1.34 mL solution of Grb2-SH2 (13.6 μM). Saturation of binding sites is observed for titrations beyond 55 min. The flat baseline at 0.0 μcal/s was obtained from the raw data by subtracting a computed baseline for each injection utilizing the pre- and postinjection data. (Bottom) Integrated values for heats of reaction normalized by the amount of ligand injected (kcal/mol of peptide) vs molar ratio of pY317−Grb2-SH2. Data were corrected for heats of dilution by subtracting a blank titration performed by injecting an equivalent amount of the pY317 peptide solution into the sample cell containing buffer only. The solid line is the best fit to the data for a single binding site model using a nonlinear least squares fit to solve for n (number of binding sites), K_b (equilibrium binding constant), and ΔH (change in enthalpy of reaction): $n = 0.961 \pm 0.007$, $K_b = (4.21 \pm 0.41) \times 10^6$ M^{-1} ($K_d = 0.24$ μM), $\Delta H = -8.02 \pm 0.08$ kcal mol^{-1}. Buffer: 50 mM Hepes, 0.15 M NaCl, pH 7.5 at 20 °C.

involved the addition of 20 10 μL injections which enabled 50% saturation to occur by the tenth injection. The heats of dilution, obtained by titrating the identical peptide solution into the reaction cell containing only the sample buffer, were subtracted prior to analysis. Heats of dilution were typically −0.05 μcal/s, and were similar to those seen in the 19th and 20th titrations in Figure 1 (top). The syringe mixing speed was 400 rpm as recommended by the vendor, and data were recorded at the 20% reference offset in order to maximize the signal-to-noise ratio. The temperature-dependent binding studies were conducted after the instrument had been equilibrated overnight at the required temperature. Nonlinear least squares analysis of the binding curve was performed using the ITC fitting algorithm included with the instrument (ITC Origin program, V2.8, MicroCal, Northampton, MA). The data fit well to a single binding site mechanism. Sufficient sample was prepared to conduct three separate titrations whose averaged values are reported here.

Computational Methods. Calculations were performed on Silicon Graphics Indigo2 or Challenge computers running the IRIX 5.x operating system. Energy minimizations were performed with the Insight II/DISCOVER program (release 2.3.5, 1994, Biosym/MSI) using the cvff force field except for the phosphotyrosine. A −2 charge on the phosphate was assumed, and partial charges were assigned using Mulliken/MNDO with the SPARTAN V3.0 (Wavefunction, Inc., 1994) program. The overall charges were +2 for the protein and −2 for the peptide.

Three pairs of homology models of the Grb2-SH2 domain (one ligand free and one peptide-containing complex) were built using the Homology (release 2.3.5, 1994, Biosym/MSI), Consensus (release 2.3.5, 1994, Biosym/MSI), and LOOK (Version 2.0beta, 1995, Molecular Applications Group) modeling programs. The crystal structures of the *Syp* (Lee *et al*., 1994a) and *Src* (Waksman *et al*., 1993) SH2 domains were used as homology templates, and the Grb2-SH2 sequence was aligned using the primary sequence-to-structural assignments of Lee *et al.* (1994a). The peptide extracted from the *Syp* cocrystal structure was used as a template to build the bound conformation of the pY317 peptide. Initial docking of this peptide to the SH2 domain models was guided by the ligand interactions described for the *Syp* and *Src* complex structures and by reported interactions between the ligand asparagine residue and the Grb2-SH2 structure (Pavlovsky *et al*., 1995). During minimization of the models for each complex, constraints were used between the pTyr of the peptide and Ser βB7, Arg βB5, and His βD4 of the protein and between the Asn(+2) of the peptide and Lys βD6 and Leu βE4 of the protein.

Solvent accessible surface areas were calculated using a 1.4 Å probe with the Biosym SOLVATION module (Delphi and Solvation User Guide, release 2.3.5, 1994, Biosym/MSI) and programs developed locally. The conformation of the free peptide was modeled by energy minimizing the template peptide in a 10 Å bath of explicit water.

Following rigid-body docking of the peptide, minimization of the complex structures included a 2 kcal mol^{-1} Å^{-2} penalty for distances greater than 5 Å between the following pairs of atoms: Ser βB7 HG−peptide P, Arg βB5 NH1−peptide P, Arg βB5 NH2−peptide P, His βD4 CB−peptide Tyr CZ, His βD4 CB−peptide Tyr CG, Lys βD6 HN−peptide Asn OD1, and Leu βE4 O−peptide Asn ND2.

To estimate the configurational contribution to ΔS of binding using the approach of Lee *et al.* (1994), it is necessary to calculate the surface areas of free, bound, and extended surface areas of individual side chains on the peptide as well as the protein. Conformations for the extended side chains (Xaa) were modeled by minimizing Ala-Xaa-Ala in a 10 Å bath of explicit water.

RESULTS

Binding Thermodynamics of Native Ligand. A thermodynamic description for the binding of the pY317 phosphotyrosine hexapeptide (Ac-SpYVNVQ-NH$_2$) to the Grb2-SH2 domain was determined using isothermal titration calorimetry. Figure 1 (top) shows the heat of reaction for 20 titrations of pY317 into a solution of Grb2-SH2. The binding reaction is exothermic, and the integrated heats of reaction for the data in Figure 1 (top) are shown as a binding curve in Figure 1 (bottom). A nonlinear least squares fit of the binding curve provides values for the stoichiometry of binding (n, ligand:protein), equilibrium binding constant (K_b), and change in enthalpy (ΔH). A thermodynamic description of binding is obtained from these parameters including the free energy of binding, ΔG, and change in entropy of reaction, ΔS:

$$\Delta G = -RT \ln(K_b) \quad (1)$$

$$\Delta G = \Delta H - T\Delta S \quad (2)$$

where R is the gas constant and T is the temperature in Kelvin.

Table 1: Thermodynamic Parameters for the Binding of Shc Peptide pY317 to Grb2-SH2

temp (°C)	K_b (10^{-6} M^{-1})	K_d (μM)	ΔG (kcal mol^{-1})	ΔH (kcal mol^{-1})	$-T\Delta S$ (kcal mol^{-1})	ΔS (cal mol^{-1} K^{-1})
15	6.06 (1.78)	0.17	−8.92 (0.16)	−6.99 (0.32)	−1.93 (0.47)	6.7 (1.6)
20	5.31 (1.05)	0.19	−9.01 (0.12)	−7.55 (0.43)	−1.46 (0.55)	5.0 (1.9)
25	4.92 (0.14)	0.20	−9.12 (0.02)	−7.94 (0.15)	−1.18 (0.15)	4.0 (0.5)
30	4.32 (0.64)	0.23	−9.20 (0.09)	−9.13 (0.22)	−0.06 (0.28)	0.2 (0.9)
35	4.73 (0.41)	0.21	−9.41 (0.06)	−9.86 (0.37)	+0.45 (0.42)	−1.5 (1.4)

[a] Binding studies were performed using pY317 (Ac-SpYVNVQ-NH_2) in 50 mM Hepes and 0.15 M NaCl, pH 7.5. The reported values are the average of three experiments and the errors represent ±1 SD. The stoichiometry, *n*, was also fit and had values between 0.9 and 1.1 for each analysis.

The solid line shown in Figure 1 (bottom) is the best fit for one of the reactions performed at 20 °C, and a summary of the average binding parameters for triplicate reactions, including the dissociation constant (K_d), is presented in Table 1. These data show that the free energy of binding (ΔG = −9.01 kcal mol^{-1}) is favored by both enthalpic (ΔH = −7.55 kcal mol^{-1}) and entropic contributions ($-T\Delta S$ = −1.46 kcal mol^{-1}).

The total heat of reaction recorded during ligand binding is derived from all processes that contribute heat to the system. For this reason the observed enthalpy of reaction (ΔH) is composed of the ligand binding heat of reaction (ΔH_{react}) and other factors. A frequent contribution to ΔH is the heat arising from the buffer due to protonation and deprotonation events during the binding step. This nonspecific buffer contribution is usually referred to as the heat of ionization (ΔH_{ion}). With this term the observed ligand binding heat of reaction can be described as

$$\Delta H = \Delta H_{react} + n_{H^+}\Delta H_{ion} \quad (3)$$

where n_{H^+} is the number of protons contributing to the reaction.

To elucidate the contribution of ΔH_{ion} and the value of n_{H^+}, we performed the binding reaction at pH 7.5 in two additional buffer systems and examined the relationship between the value of ΔH with respect to the known heat of reaction for all three buffers (Christensen *et al*., 1976; Murphy *et al*., 1993; Gomez & Freire, 1995). This relationship is presented in Figure 2, and the results show that the value of ΔH, at pH 7.5, is independent of ΔH_{ion} of the buffer. Thus, the binding reaction of pY317 with Grb2-SH2 occurs in the absence of a significant protonation event, i.e. $n_{H^+} \sim 0$, and that $\Delta H = \Delta H_{react}$.

Temperature Dependence of Ligand Binding: ΔC_p of Binding. Titrations were also performed between 15 and 35 °C to determine the change in heat capacity, ΔC_p, upon ligand binding. ΔC_p was calculated from the dependence of ΔH_{react} on temperature (Table 1 and Figure 3) and based on the slope has a value of −146 cal mol^{-1} K^{-1}. The size and sign of ΔC_p are consistent with a binding interaction that involves a net increase in buried apolar surface area.

A summary of the temperature-dependent thermodynamics of binding is shown in Table 1 and Figure 3. These values indicate that while the ΔG of binding becomes slightly more favorable (5%) with increasing temperature, the enthalpy contribution becomes much more favorable (∼40%). This favorable increase in enthalpy is nearly completely offset by unfavorable entropic effects. For example, at 15 °C ΔH = −6.99 kcal mol^{-1} and $-T\Delta S$ = −1.93 kcal mol^{-1}, while the values at 35 °C are ΔH = −9.86 kcal mol^{-1} and $-T\Delta S$ = +0.45 kcal mol^{-1}.

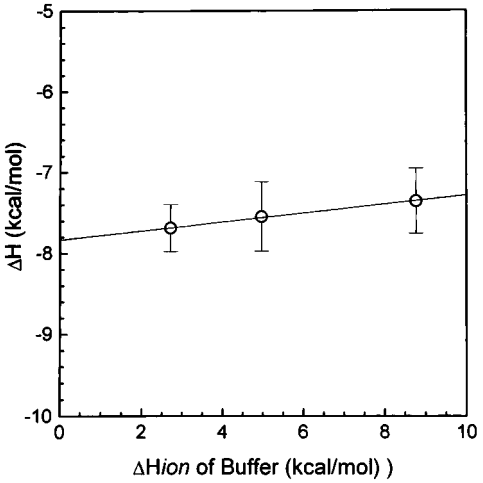

FIGURE 2: Estimate of the ligand binding induced heat of ionization. The observed reaction enthalpies are plotted vs heats of ionization for three different buffers. The slope of the line, which is proportional to the degree of protonation or deprotonation upon ligand binding, is 0.05 and indicates that pY317 binding is not coupled to a protonation reaction. Buffers: PIPES, ΔH_{ion} = 2.72 kcal mol^{-1}; Hepes, ΔH_{ion} = 4.97 kcal mol^{-1}; imidazole, ΔH_{ion} = 8.77 kcal mol^{-1}. Reactions were performed in 50 mM buffer, 0.15 M NaCl, pH 7.5 at 20 °C.

pY317 Polypeptide Side Chain Contributions to Binding: Alanine Substitutions. The specificity for ligand binding to Grb2-SH2 requires phosphotyrosine and asparagine, with a consensus primary sequence of pY-X-N-X. However, the individual contributions of pY and N to the energetics of binding are unclear. In addition, the contribution of the side chains for the remaining residues (X) is also unknown. To identify the thermodynamic contributions of binding by each of the side chains in the pY317 ligand, we performed additional binding studies using five different peptides containing a single alanine substitution for each of the native residues.

A summary of thermodynamic binding parameters for the alanine-substituted peptides is presented in Table 2. Starting from the N-terminus of the peptide, we determined that there was no significant difference in the thermodynamics of binding for the serine-to-alanine substituted ligand, S(−1)A. This was consistent with the molecular model of the complex which showed minimal interactions between the side chain of serine and Grb2-SH2 (see homology modeling section and Figure 5). We could not perform binding studies with the alanine-substituted phosphotyrosine (pY/A) ligand due to its low solubility and weak affinity. However, from a limited binding study we determined that the affinity of the more soluble ligand NH_2-SYVNVQ-COOH (unblocked N- and C-terminus and containing a tyrosine residue) was very weak (K_d ∼1−10 mM).

The thermodynamics of binding for the V(+1)A peptide was unexpected. The favorable entropic contribution to

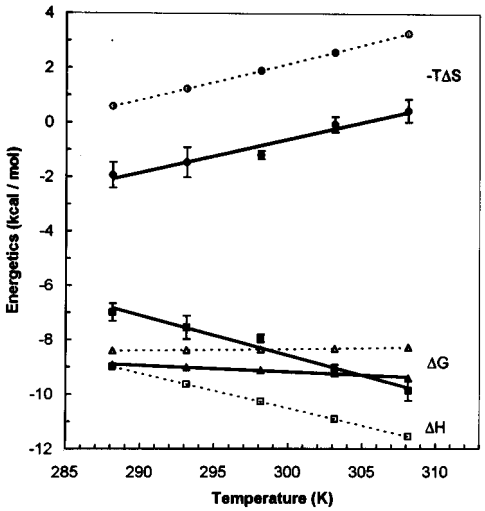

FIGURE 3: Temperature-dependent energetics of binding for Grb2-SH2 and pY317: comparison of computed and experimentally determined thermodynamic binding parameters. The experimental data, ΔH (solid squares), $-T\Delta S$ (solid circles), and ΔG (solid triangles), are shown along with a solid line representing a linear least squares fit to the data which assumes a linear temperature dependence (see Table 1). The heat capacity of binding (ΔC_p), determined from the slope for ΔH, has a value of -146 cal mol^{-1} K^{-1}. ITC binding reactions were performed from 15 to 35 °C at 5 °C intervals under solution conditions described in Figure 1. The LOOK homology model structure-based values for ΔH, $-T\Delta S$, and ΔG, derived from eqs (1, 2, 4, 5, and 6), are shown as thin dotted lines with open symbols corresponding to the experimental data (see Tables 3 and 4). Error bars represent standard deviations from three experiments.

binding seen in the native substrate, pY317 ($-T\Delta S = -1.46$ kcal mol^{-1}, Table 2), becomes unfavorable for the V(+1)A substitution ($-T\Delta S = +0.81$ kcal mol^{-1}). The sign and magnitude of the $\Delta\Delta H$ and $-\Delta T\Delta S$ values (-1 and $+2.27$ kcal mol^{-1}, respectively) for the V(+1)A peptide are consistent with the release of an ordered water molecule upon binding of the native peptide (Dunitz, 1993). Presumably when the alanine-substituted peptide is bound, both the alanine methyl group and water molecule can simultaneous occupy a surface pocket.

The substitution of alanine for asparagine, N(+2)A, resulted in a large, 2000-fold, decrease in affinity ($\Delta G = -4.62$ kcal mol^{-1}). The total decrease in free energy of binding ($\Delta\Delta G$) relative to the native substrate (pY317) was +4.39 kcal mol^{-1} and was primarily due to a loss in favorable enthalpy contributions ($\Delta\Delta H = +5.6$ kcal mol^{-1}). The importance of asparagine in binding is consistent with its strict conservation in the sequence of native ligands, and the calorimetric results with the alanine-substituted peptide presumably reflect a loss in hydrogen-bonds between the asparagine side chain and Grb2-SH2 (Figure 5). Despite the loss in enthalpic contributions, the association remained entropically favorable ($-T\Delta S = -2.67$ kcal mol^{-1}) .

Substitution of the second valine V(+3)A caused a slight decrease in ΔG which is due to a decrease in favorable enthalpic interactions ($\Delta\Delta H = +1.58$ kcal mol^{-1}). Finally, the thermodynamics of binding for the Q(+4)A substrate and the native ligand are nearly identical. This implies that the glutamine side chain is not critical for complex formation. Taken together, these analyses have identified the side chains of pY, V(+1), and N(+2) as the most critical for binding of the Shc peptide to Grb2-SH2.

Homology Modeling of the Grb2-SH2−pY317 Complex. To enable an evaluation of the molecular interactions on the surface of the SH2 domain that would promote ligand binding and to compute binding parameters for comparison to experimentally observed values, homology models of the Grb2-SH2 domain were constructed. The three homology models were built using different methodologies. The *Consensus* model was generated using distance geometry methods (Havel & Snow, 1991) with distance constraints derived from previously determined homology structures. The *Homology* model used traditional methodology (Greer, 1981) where the structurally conserved regions were built from homologous structures and the loops were modeled from a larger database of loop conformations. The *LOOK* model was constructed using an automated segment algorithm and a database of highly refined known structures (Levitt *et al*., 1992).

All of the homology models have the same overall topology (Figure 4). The Cα RMS differences for secondary structural elements are 1.51 Å (LOOK vs Homology), 1.61 Å (LOOK vs Consensus) and 1.74 Å (Consensus vs Homology). Pairwise RMS deviations for complex models are 1.62, 1.62, and 1.46 Å, respectively. Differences between the models are in the BG loop and, to a lesser extent, in the BC loop and the C-terminus beyond Glu βG3 (Figure 4). While the differences in the BG loop conformation alter the structure of the Asn(+2) site, the putative interactions of Asn(+2) with the backbone of Lys βD6 and Leu βE4 (Figure 5) were similar in the three models. As expected, the phosphotyrosine site in this model is very similar to the phosphotyrosine binding site in the *Syp* (Lee *et al*., 1994a) and *Src* (Waksman *et al*., 1993) structures on which the model is based (Figure 5). The phosphate group interacts with Ser βC3, Arg βB5, Ser BC2, Ser βB7, and the backbone of Glu BC1. The Asn side chain at +2 forms hydrogen bonds with the side chain of Lys βD6 and backbone carbonyl of Leu βE4 (Figure 5). The Cα RMS deviations between the SH2 domain in the unliganded and liganded forms are 1.14 Å for the model built with LOOK and 1.27 Å for the Consensus and 1.14 Å for the Homology models. After

Table 2: Thermodynamic Parameters for the Binding of Native and Alanine-Substituted Shc Peptides to Grb2-SH2[a]

peptide	K_d (μM)	ΔG (kcal mol^{-1})	ΔH (kcal mol^{-1})	$-T\Delta S$ (kcal mol^{-1})	ΔS (cal mol^{-1} K^{-1})
Ac-S-pY-V-N-V-Q-NH_2	0.19	−9.01 (0.12)	−7.55 (0.43)	−1.46 (0.55)	5.0 (1.9)
Ac-**A**-pY-V-N-V-Q-NH_2	0.20	−8.95 (0.13)	−7.19 (0.37)	−1.75 (0.50)	6.0 (1.7)
Ac-S-pY-**A**-N-V-Q-NH_2	1.63	−7.73 (0.05)	−8.54 (0.01)	+0.81 (0.06)	−2.8 (0.2)
Ac-S-pY-V-**A**-V-Q-NH_2	359.	−4.62 (0.08)	−1.95 (0.02)	−2.67 (0.07)	9.1 (0.2)
Ac-S-pY-V-N-**A**-Q-NH_2	0.77	−8.17 (0.08)	−5.97 (0.19)	−2.21 (0.27)	7.5 (0.9)
Ac-S-pY-V-N-V-**A**-NH_2	0.30	−8.72 (0.11)	−7.14 (0.56)	−1.58 (0.67)	5.4 (2.3)

[a] Binding studies were performed in 50 mM Hepes and 0.15 M NaCl, pH 7.5 at 20 °C. The reported values are the average of three experiments except for line 4, which is from two experiments. The reported K_d values were calculated from the K_b values which were fit directly from the binding analysis. The errors represent ±1 SD. The stoichiometry, *n*, was also fit and had values between 0.9 and 1.1 for each analysis.

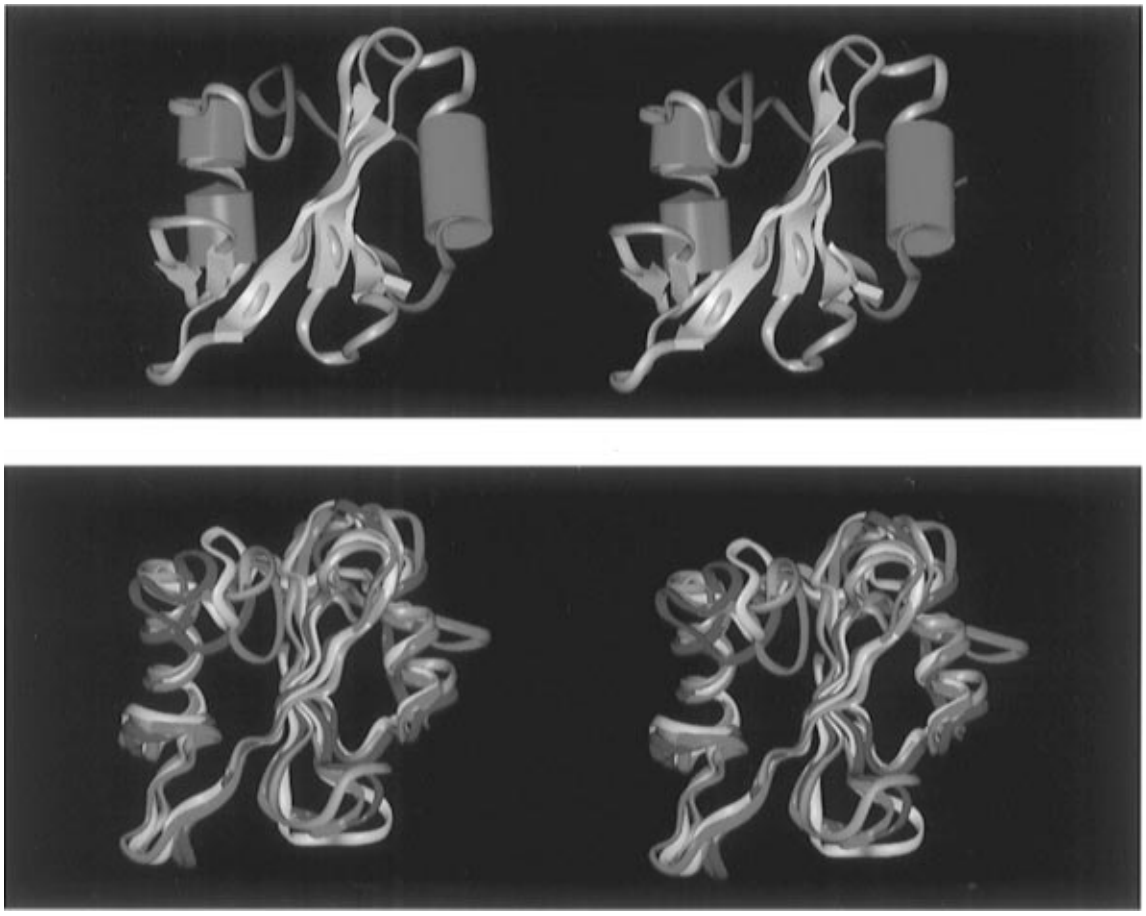

FIGURE 4: Structure of Grb2-SH2 domain. (A, top) Stereo diagram of the LOOK model. The following Grb2-SH2 structural elements are shown in the figure from right to left: N-terminus, βA, αA, βB, βC, β(D−D′), βE, βF, α(B−B′) − βG(β strand not shown), and C-terminus. The N- and C-terminal polypeptide regions are colored blue and red, respectively. The helices and β-strands are colored green and yellow, respectively. Strands A−D form the central β-sheet. (B, bottom) Superposition of the LOOK (green), Consensus (orange), and Homology (purple) models and the crystallographically determined structure (yellow) (Maignan *et al*., 1995).

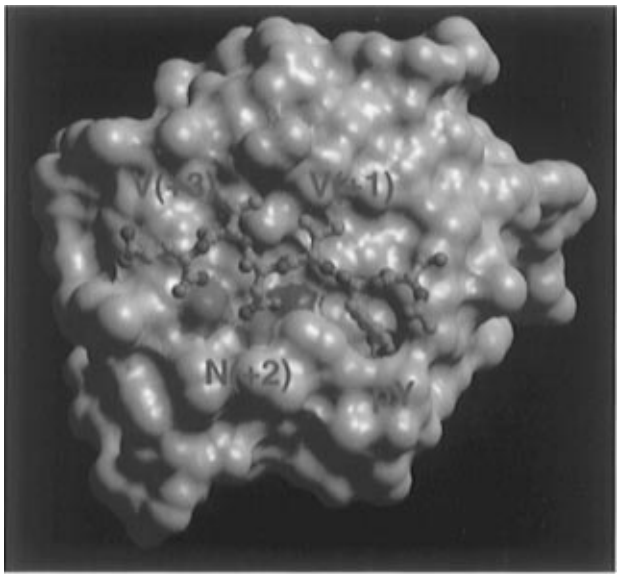

FIGURE 5: LOOK-derived model of the interaction between the pY317 peptide ligand and the Grb2-SH2 domain. The solvent-accessible surface is colored to illustrate the hydrogen bonds with Asn(+2). The SH2 backbone amide NH is blue and carbonyl O atoms of Lys βD6 and Leu βE4 are red. As expected, the phosphotyrosine site in this model is very similar to that of the structures on which the model is based (Lee *et al*., 1994a; Waksman *et al*., 1993). The phosphate group interacts with Ser βC3, Arg βB5, Ser BC2, Ser βB7, and the backbone of Glu BC1.

completion of this work, the crystallographic coordinates of the uncomplexed Grb2-SH2 domain were released (Maignan et al., 1995). The Cα RMS differences for secondary structural elements between the crystal structure and the homology models are 1.54 Å (Consensus), 1.74 Å (Homology), and 1.29 Å (LOOK) (Figure 4B). The largest structural differences occur in the BG loop and the C-terminus (Figure 4B).

Structure-Based Semiempirical Estimates of Thermodynamic Binding Parameters. The value of ΔC_p associated with peptide−protein interactions as well as the ΔH and the solvent contribution to the total entropy term, ΔS_{solv}, can be approximated, from the three-dimensional structure of the protein−ligand complex, as a simple function of the change in the polar and apolar surface areas associated with the binding event (Murphy & Freire, 1992; Spolar *et al*., 1992; Murphy *et al*., 1993; Gomez & Freire, 1995; Myers *et al*., 1995). According to Freire and coworkers, the relationship between ΔC_p and the solvent accessible surface area is

$$\Delta C_p = 0.45\Delta\mathrm{ASA}_{\mathrm{apol}} - 0.26\Delta\mathrm{ASA}_{\mathrm{pol}} + \Delta C_{p,\mathrm{ion}} \quad (4)$$

where $\Delta\mathrm{ASA}_{\mathrm{apol}}$ and $\Delta\mathrm{ASA}_{\mathrm{pol}}$ are the changes in accessible surface area upon binding for apolar and polar residues, respectively. $\Delta C_{p,\mathrm{ion}}$ is the heat capacity change due to protonation and deprotonation reactions coupled to the ligand binding step. Since the value of n_{H^+} for Grb2 is nearly 0 at pH 7.5, as shown above, the value for $\Delta C_{p,\mathrm{ion}}$ is also 0.

Table 3: Solvent Accessible Surface Areas and Structure-Based Semi-Empirical Estimates of ΔC_p

	homology models[a]			experimental results[b]
	Homology	Consensus	LOOK	
ASA_{pol} Grb2 (Å^2)	2307	2174	2270	
ASA_{apol} Grb2 (Å^2)	3777	3511	3620	
ASA_{pol} pY317 (Å^2)	586	586	586	
ASA_{apol} pY317 (Å^2)	636	636	636	
ASA_{pol} complex (Å^2)	2161	2350	2208	
ASA_{apol} complex (Å^2)	3563	3676	3597	
ΔASA_{pol} (Å^2)	−731	−410	−647	−609
ΔASA_{apol} (Å^2)	−851	−471	−659	−677
ΔC_p (cal mol^{-1} K^{-1})	−193	−106	−128	−146

[a] The homology model-derived values for ΔASA_{pol} and ΔASA_{apol} were calculated using complex − (Grb2 + pY317) ASA values for the polar and apolar surfaces, respectively. The value of ΔC_p for the homology models was calculated using eq 4. Abbreviations: Grb2, unliganded structure of Grb2-SH2; pY317, structure of the pY317 ligand; complex, structure of the Grb2-SH2 + pY317 complex. [b] The experimentally derived values for ΔASA_{pol} and ΔASA_{apol} were calculated using the equations from Murphy and Freire (1992) as described in the text (eqs 4 and 5).

A similar relationship was observed between the value of the change in enthalpy at 60 °C, $\Delta H(60)$, and the accessible surface area:

$$\Delta H(60) = (31.4\Delta ASA_{pol} - 8.44\Delta ASA_{apol}) + \Delta H_{ion} \quad (5)$$

where the value of ΔH_{ion} has been determined to be 0 at pH 7.5.

Methods to estimate the total entropic contribution, ΔS, involve summation of entropic changes due to solvation (ΔS_{solv}), configurational (ΔS_{conf}), ionization (ΔS_{ion}) and rotational/translational (ΔS_{rt}) contributions as shown in the following equation:

$$\Delta S = \Delta S_{solv} + \Delta S_{conf} + \Delta S_{ion} + \Delta S_{rt} \quad (6)$$

The solvent contribution (or hydrophobic effect), ΔS_{solv}, was estimated from the relationship: $\Delta S_{solv} = \Delta C_p \ln(T/385.15)$. In addition, ΔS_{conf} was calculated on the basis of the work of Lee et al. (1994b), and ΔS_{ion} was experimentally determined to be 0 (see above). Also, given the 1:1 binding stoichiometry, we assume a value of −8 cal K^{-1} mol^{-1} for the change in overall rotational/translational entropy, ΔS_{rt} (Murphy et al., 1993).

The calculated structure-based values of ΔASA_{pol} and ΔASA_{apol} for each homology model are presented in Table 3. The results demonstrate that the ligand binding event involves the burial of nearly equal amounts of polar and apolar surface areas (e.g., LOOK-derived values of ΔASA_{pol} and ΔASA_{apol} are −647 and −659 Å^2, respectively). Using the experimentally derived values of ΔC_p and ΔH and eqs 4 and 5 we calculated experimental values for ΔASA_{pol} and ΔASA_{apol}. We obtained values of −609 and −677 Å^2 for ΔASA_{pol} and ΔASA_{apol}, respectively (Table 3), which suggests that ligand binding involves nearly identical extents of burial for polar and apolar surfaces and this result is consistent with the homology model results.

The methodology, equations, and values described above were used to estimate structure-derived values of ΔC_p, as well as ΔH, ΔS, and ΔG values of binding as a function of temperature (Tables 3 and 4 and Figure 3). The calculated values were then compared to the results obtained by isothermal titration calorimetry (Table 1 and Figure 3). While none of the models quantitatively reproduces the experimental results, all correctly reproduce the trends that binding is enthalpically favored and that the entropic effects of complex formation are small. Further, since the correct sign and approximate magnitude for ΔC_p can be calculated from the models, the temperature dependence of both the entropy and enthalpy of binding is modeled correctly.

We selected the LOOK models for more extensive comparison to the experimentally-derived information because calculated values derived from these structures showed slightly better agreement with the experimental ΔC_p and ΔG of binding, and with the surface area changes estimated from the calorimetric data (see Discussion).

DISCUSSION

A thermodynamic analysis for the binding of a phosphotyrosine peptide from Shc protein (pY317) to the SH2 domain of Grb2 has been conducted using isothermal titration calorimetry, and the experimental results have been compared to values calculated using three-dimensional homology models of the Grb2-SH2 domain. The results from ITC experiments indicated the binding reaction occurred with a stoichiometry of one pY peptide to one SH2 domain with $\Delta G = -9.0$ kcal mol^{-1} at 20 °C. This interaction was both enthalpically ($\Delta H = -7.55$ kcal mol^{-1}) and entropically ($-T\Delta S = -1.46$ kcal mol^{-1}) favored. The corresponding

Table 4: Structure-Based Semiempirical Estimates of ΔH, ΔS, and ΔG[a]

	homology models			experimental results
	Homology	Consensus	LOOK	
$\Delta H_{binding}$ (kcal/mol)	−8.06	−4.66	−9.61	−7.55
ΔH_{ion} (kcal/mol)	0	0	0	0
total ΔH (20 °C, kcal/mol)	−8.06	−4.66	−9.61	−7.55
ΔS_{solv} (cal mol^{-1} K^{-1})	53	29	35	40
ΔS_{rt} (cal mol^{-1} K^{-1})	−8	−8	−8	
ΔS_{conf} (cal mol^{-1} K^{-1})	−29	−31	−31	
ΔS_{ion} (cal mol^{-1} K^{-1})	0	0	0	0
total ΔS (20 °C, cal mol^{-1} K^{-1})	16	−10	−4	5
total $-T\Delta S$ (20 °C, kcal mol^{-1})	−4.59	3	1.2	−1.46
total ΔG (20 °C, kcal mol^{-1})	−12.66	−1.66	−8.4	−9.01

[a] All values are for 20 °C. The ΔH structure-based values for the homology models were calculated using the ΔASA values reported in Table 3 and eq 5 from the text (Murphy & Freire, 1992; Murphy *et al.*, 1993). The ΔH values were corrected to 20 °C using the ΔC_p value from eq 4 and the equation: $\Delta H(20) = \Delta H(60) - 40\Delta C_p$. Entropy values were calculated as described in the text (eq 6), as well as by Gomez and Freire (1995) and Lee *et al.* (1994).

dissociation constant (K_d) is 0.19 μM and is similar to the K_d (0.38 μM) measured by Lemmon *et al*. (1994) for binding of a related peptide (EGF-R, PVPpY$_{1068}$INQSVPKRK) to the intact SH3−SH2−SH3 Grb2 molecule. Thus, the similar affinity of peptides for the isolated SH2 domain and the intact SH3−SH2−SH3 molecule suggests that peptide binding to the SH2 domain is relatively independent of the SH3 domains. Lemmon and Ladbury (1994) also observed nearly identical affinities and enthalpies for phosphotyrosine polypeptides binding to constructs of the *lck* SH2 protein containing either the two-domain SH3−SH2 (63−228) protein or the isolated SH2 (123−228) domain. These results are consistent with the recently determined three-dimensional structure of the full-length Grb2 molecule (SH3−SH2−SH3) which shows three loosely associated domains (Maignan *et al*., 1995).

The binding study by Lemmon *et al*. (1994), using the intact Grb2 molecule (SH3−SH2−SH3) to determine the affinity of the pY peptide, was performed using the surface plasmon resonance technique because ITC measurements using their peptide apparently generated low values of ΔH ($\sim$−1 kcal mol^{-1}). This result is surprising since our pY317 peptide gave a large value of ΔH (−7.55 kcal mol^{-1}). Cussac *et al*. (1994) used fluorescence enhancement techniques to measure the affinity of Grb2 ligands. These studies showed that peptide ligands containing sequences similar to those used in our study (Shc, PSpY$_{317}$VNVQN; and human growth factor receptor, ATpY$_{1374}$VNVKS) had K_d values of 18 and 80 nM, respectively. In both studies, differences in measured affinities could reflect variations in either the length or composition of the peptide ligands or, in the latter case, differences in phosphotyrosine molar extinction coefficient used for concentration determinations.

The alanine substitution study reported here shows that binding of the native peptide is favored by enthalpic contributions arising primarily from the phosphotyrosine and the N(+2) residues. A significant portion of the phosphotyrosine contribution may reside in the phosphate moiety since preliminary studies indicate that the tyrosine-containing ligand (NH_2-SYVNVQ-COOH) had a K_d of only $\sim$1−10 mM and a low value of ΔH, $\sim$−1 kcal mol^{-1} (data not shown). The large decrease in affinity and low value of ΔH for the NH_2-SYVNVQ-COOH peptide is consistent with the loss of an extensive network of hydrogen bonds to the phosphate moiety as is typically seen in peptide−SH2 domain structures. In the LOOK complex model, for example, there are nine hydrogen bonds between the pY and the protein. Although the phosphate group is critical for high affinity of the pY-containing polypeptides, a phosphotyrosine amino acid residue alone exhibits poor binding affinity, K_d $\sim$1−5 mM (Lemmon & Ladbury, 1994; Burke *et al*., 1995).

Results from the alanine scanning experiments are consistent with the homology models. Substitution of the N(+2) residue for alanine decreased the affinity $\sim$2,000-fold. The lower affinity (K_d $\sim$0.36 mM) reflects decreases in ΔH of binding from −7.55 kcal mol^{-1} for N(+2) to −1.95 kcal mol^{-1} for N(+2)A. The large changes in both the affinity and enthalpy of binding for the N(+2)A ligand are consistent with the loss of two hydrogen bonds between the asparagine side chain and the Lys βD6 backbone amide proton and Leu βE4 backbone carbonyl (Figure 5).

Perhaps the most interesting and unexpected observation pertains to the thermodynamic binding properties for the V(+1)A peptide. The calorimetric data for the native and alanine-substituted peptide are consistent with displacement of a water molecule by the valine side chain (Dunitz, 1993). The observed preference for hydrophobic residues by Grb2 at the (+1) site likely reflects their ability to displace bound solvent molecules. In the homology models, Gln βD3 is positioned such that it could play a role in ordering the water molecule. Together, these data could easily be incorporated into a structure-based drug design cycle. In contrast, the V(+3)A peptide shows neither the appropriate changes in the thermodynamics of binding nor appropriate binding sites on the surface of the model for a water molecule to be displaced by V(+3) upon binding. This result is consistent with the wide range of residues tolerated at the (+3) site. These thermodynamic and structural studies are consistent with a Grb2-SH2 recognition motif of pY-hydrophobic-N-X (where X is any amino acid).

The accuracy of three-dimensional homology models depends on the extent of sequence homology, the degree of structural conservation, and the availability of experimental constraints to ensure accurate representation of the binding site. The high sequence homology and structural conservation among SH2 domains give confidence that the models used here are accurate. In this case, construction of the peptide−SH2 domain complex was additionally guided by a short communication (Pavlovsky *et al*., 1995) describing the intermolecular hydrogen bonds between the N(+2) side chain and Grb2-SH2 domain. Here we propose that construction of homology models be additionally evaluated by the agreement between experimentally measured and calculated thermodynamic parameters associated with ligand binding reactions. As shown in Tables 3 and 4, values of ΔC_p and ΔH depend on the homology model used in the calculation. An evaluation of the data in these tables shows that the values calculated using the model built with LOOK are closest to those observed experimentally.

At a qualitative level, calculations using each of the models provided ΔC_p values (−106 to −193 cal mol^{-1} K^{-1}) well within the range of the experimentally determined value of −146 cal mol^{-1} K^{-1}. The models also predict enthalpically favored peptide binding (Table 4). Although the magnitude of the entropic contribution to binding is model dependent, all models correctly predict that the entropic contribution is small compared to the enthalpic contribution. Similarities between the value and temperature dependence of the model-dependent and experimentally derived results are apparent in Figure 3.

Two other groups have derived similar semiempirical functions relating ΔC_p to a function of ΔASA_{apol} and ΔASA_{pol}. Spolar *et al*. (1992) developed eq 7 and Myers *et al*. (1995) recently developed eq 8. The ΔC_p values

$$\Delta C_p = 0.31(\Delta ASA_{apol}) - 0.14(\Delta ASA_{pol}) \quad (7)$$

$$\Delta C_p = 0.28(\Delta ASA_{apol}) - 0.09(\Delta ASA_{pol}) \quad (8)$$

calculated from eq 7 and 8 using the solvent-accessible surface areas from the LOOK model (Table 4) are −125 and −130 cal mol^{-1} K^{-1}, respectively. Both agree with the values of −128 cal mol^{-1} K^{-1} calculated using eq 4 (Murphy & Freire, 1992; Murphy *et al*., 1993) and the measured −146 cal mol^{-1} K^{-1}. The low values of ΔC_p determined either by experimentation or from the homology models and the corresponding accessible surface areas are consistent for a binding interaction which involves the burying of nearly equal amounts of polar and apolar surface areas (Table 3).

In conclusion, we have demonstrated that phosphotyrosine-dependent binding to the Grb2-SH2 domain is favored by enthalpic contributions arising primarily from the pY and N(+2) residues and that significant entropic contributions arise from V(+1). On the basis of the comparison of the thermodynamics of binding and the homology models, it appears that design of a small molecule antagonist with specificity targeting the Grb2-SH2 domain should include the pY, V(+1), and N(+2) ligand binding sites (Figure 5). In addition, we have shown that the thermodynamics of binding a short phosphotyrosine polypeptide can be calculated with moderate success using the empirical formulations relating ligand affinity to the change in accessible surface areas for apolar and polar atoms upon complex formation.

ACKNOWLEDGMENT

We are grateful to Stuart Black and Dr. Oswald Wilson for the expression of Grb2-SH2, Dr. Anne Frederick for contributing to the Grb2-SH2 modeling studies, and Dr. Nicholas Murgolo for discussions regarding SH2 structures.

REFERENCES

Burke, T. R., Barchi, J. J., George, C., Wolf, G., Shoelson, S. E., & Yan, X. (1995) *J. Med. Chem. 38*, 1386−1396.

Christensen, J. J., Hansen, L. D., & Izatt, R. M. (1976) Handbook of Proton Ionization Heats and Related Thermodynamic Quantities, John Wiley and Sons, New York.

Cussac, D., Frech, M., & Chardin, P., (1994) *EMBO J. 13*, 4011−4021.

Dunitz, J. D. (1994) *Science 264*, 670.

Eck, M. J., Shoelson, S. E., & Harrison, S. C. (1993) *Nature 363*, 87−91.

Egan, S. E., Giddings, B. W., Brooks, M. W., Buday, L., Sizeland, A. M., & Weinberg, R. A. (1993) *Nature 363*, 45−51.

Gómez, J., & Freire, E. (1995) *J. Mol. Biol. 252*, 337−350.

Greer, J. (1991) *J. Mol. Biol. 153*, 1027−1042.

Havel, T. F. & Snow, M. E. (1991) *J. Mol. Biol. 217*, 1−7.

Ladbury, J. E., Lemmon, M. A., Zhou, M., Green, J., Botfield, M. C., and Schlessinger, J. (1995) *Proc. Natl. Acad. Sci. U.S.A. 92*, 3199−3203.

Lee, C.-H., Kominos, D., Jacques, S., Margolis, B., Schlessinger, J., Shoelson, S. E., & Kuriyan, J. (1994a) *Structure 2*, 423−438.

Lee, K. H., Xie, D., Freire, E., & Amzel, L. M. (1994b) *Proteins 20*, 68−84.

Lemmon, M. A., & Ladbury, J. E. (1994) *Biochem. 33*, 5070−5076.

Lemmon, M. A., Ladbury, J. E. Mandiyan, V., Zhou, M., & Schlessinger J., (1994) *J. Biol. Chem. 269*, 31653−31658.

Levitt, M. (1992) J. Mol. Biol. 226, 507−533.

Li, N., Baltzer, A., Daly, R., Yajnik, V., Skolnik, E., Chardin, P., Bar-Sagi, D., Margolis, B., & Schlessinger, J. (1993) *Nature 363*, 85−88.

Lowenstein, E. J., Daly, R. J., Batzer, A. G., Li, W., Margolis, B., Lammers, R., Ullrich, A., Skolnik, E. Y., Bar-Sagi, D., & Schlessinger, J. (1992) *Cell 70*, 431−442.

Maignan, S., Guilloteau, J. P., Fromage, N., Arnoux, B., Becquart, J., & Ducruix, A. (1995) *Science 268*, 291−293.

Maru, Y., Peters, K. L., Afar, D. E., Shibuya, M., Witte, O. N., & Smithgall, T. (1995) *Mol. Cell. Biol. 15*, 835−842.

Maru, Y., Witte, O. N., & Shibuya, M. (1996) *FEBS Lett. 379*, 244−246.

Murphy, K. P., & Freire, E. (1992) *Adv. Protein Chem. 43*, 313−361.

Murphy, K. P., Xie, D., Garcia, K. C., Amzel, L. M., & Freire, E. (1993) *Proteins: Struct., Funct., Genet. 15*, 113−120.

Myers, J. K., Pace, C. N., & Scholtz, J. M. (1995) *Protein Sci. 4*, 2138−2148.

Pascal, S. M., Singer, A. U., Gish, G., Yamazaki, T., Shoelson, S. E., Pawson, T., Kay, L. E., & Forman-Kay, J. D. (1994) *Cell 77*, 461−472.

Pavlovsky, A. G., Singh, J., Rubin, J. R., Humblet, C., Mueller, W. T., McConnell, P., & Slintak, V. (1995) American Crystallographic Association Annual Meeting Abstract W051.

Pawson, T. (1995) *Nature 373*, 573−580.

Pawson, T., & Schlessinger, J. (1993) *SH2 and SH3 domains*, *Curr. Biol. 3*, 434−442.

Pendergast, A. M., Quilliam, L. A., Cripe, L. D., Bassing, C. H., Dai, Z., Li, N., Batzer, A., Rabun, K. M., Der, C. J., Schlessinger, J., & Pawson, T. (1993) *Cell 75*, 175−185.

Rozakis-Adcock, M., McGlade, J., Mbamalu, G., Pelicci, G., Daly, R., Li, W., Batzer, A., Thomas, S., Brugge, J., Pelicci, P. G., Schlessinger, J., & Pawson, T. (1992) *Nature 360*, 689−692.

Rozakis-Adcock, M., Fernley, R., Wade, J., Pawson, T., & Bowtell, D. (1993) *Nature 363*, 83−85.

Sadowsky, I., Stone, J. C., & Pawson, T. (1986) *Mol. Cell. Biol. 6*, 4396−4408.

Skolnik, E. Y., Batzer, A., Li, N., Lee, C-H., Lowenstein, E., Margolis, B., & Schlessinger, J. (1993) *Science 260*, 1953−1955.

Songyang, Z., Shoelson, S. E., Chaudhuri, M., Gish, G., Pawson, T., Haser, W. G., King, F., Roberts, T., Ratnofsky, S., Lechleider, R. J., Neel, B. G., Birge, R. B., Fajardo, J. E., Chou, M. M., Hanafusa, H., Schaffhausen, B., & Cantley, L. C. (1993) *Cell 72*, 767−778.

Songyang, Z., Shoelson, S. E., McGlade, J., Oliver, P., Pawson, T., Bustelo, R., Barbacid, M., Sabe, H., Hanafusa, H., Yi, T., Ren, R., Baltimore, D., Ratnofsky, S., Feldman, R. A., & Cantley, L. C. (1994) *Mol. Cell Biol. 14*, 2777−2785.

Spolar, R. S., Livingstone, R. J., & Record, M. T., Jr. (1992) *Biochemistry 31*, 3947−3955.

Waksman, G., Kominos, D., Robertson, S. C., Pant, N., Baltimore, D., Birge, R. B., Cowburn, D., Hanafusa, H., Mayer, B. J., Overduin, M., Resh, M. D., Rios, C. B., Silverman, L., & Kuriyan, J. (1992) *Nature 358*, 646−653.

Waksman, G., Shoelson, S. E., Pant, N., Cowburn, D., & Kuriyan, J., (1993) Cell 72, 779−790.

Ward, C. W., Gough, K. H., Rashke, M., Wan, S. S., Tribbick, G., & Wang, J-X. (1996) *J. Biol.Chem. 271*, 5603−5609.

Wiseman, T., Williston, S., Brandts, J. F., & Lin, L.-N. (1989) *Anal. Biochem. 179*, 131−137.

Xu, R. X., Word, J. M., Davis, D. G., Rink, M. J., Willard, D. H., & Gampe, R. T. (1995) *Biochemistry 34*, 2107−2121.

BI9704360